Bayesian Uncertainty Quantification and Propagation (UQ+P): State-of-the-Art Tools for Linear and Nonlinear Structural Dynamics Models

Costas Papadimitriou

Abstract A Bayesian framework for uncertainty quantification and propagation in complex structural dynamics simulations using vibration measurements is presented. The framework covers uncertainty quantification techniques for parameter estimation and model selection, as well as uncertainty propagation techniques for robust prediction of output quantities of interest in reliability and safety of the structural systems analyzed. Bayesian computational tools such as asymptotic approximation and sampling algorithms are presented. The Bayesian framework and the computational tools are implemented for linear and nonlinear finite element models in structural dynamics using either identified modal frequencies, measured response time histories, or frequency response spectra. High performance computing techniques that drastically reduce the excessive computational demands that arise from the large number of system simulations are outlined. Identified modal properties from a full-scale bridge demonstrate the use of the proposed framework for parameter estimation of linear FE models.

1 Introduction

In the process of simulating the behavior of complex engineering systems, uncertainties arise mainly from the assumptions and compromises that enter into the development of mathematical models of such systems and the applied loads. Such uncertainties lead to significant uncertainties in the predictions made using simulations. Since predictions form the basis for making decisions, the knowledge of these uncertainties is very important.

The sources of uncertainties in engineering simulations are modeling uncertainties, loading uncertainties, and numerical uncertainties. Modeling uncertainties are related to the inadequacy of the mathematical model to represent a physical system. They arise in modeling the constitute behavior of materials, the support conditions

C. Papadimitriou (✉)
Department of Mechanical Engineering, University of Thessaly, Volos, Greece
e-mail: costasp@uth.gr

E.N. Chatzi and C. Papadimitriou (eds.), *Identification Methods for Structural Health Monitoring*, CISM International Centre for Mechanical Sciences 567,
DOI 10.1007/978-3-319-32077-9_6

of structures and their interaction with their environment, the interaction/coupling between substructures (fixity conditions, friction mechanisms, impact phenomena), the geometric variability due to manufacturing/construction processes, the long-term deterioration mechanisms (e.g., semiempirical models for fatigue and corrosion), etc. The parametric uncertainties, originating in the limited knowledge about the values of the model parameters, are also considered as part of the modeling uncertainties. Loading uncertainties arising from the lack of detailed knowledge of the spatial and temporal variation of the forces (mechanical, thermal, etc.) applied to engineering structures. Representative examples of loading uncertainties in structural dynamics include spatial variability of road roughness affecting the dynamics of vehicles, spatial and temporal variability of wind or earthquake-induced excitations on civil engineering structures, turbulent wind loads affecting the design and maintenance of aircrafts, variability of thermal loads affecting the design of a large class of mechanical and aerospace structures. Numerical uncertainties are related to the spatial (e.g., finite element) and temporal (numerical time integration schemes) discretization of the partial differential equations used for simulating the behavior of engineering structures, round-off errors due to computer accuracies, all affecting solution accuracy.

Probability distribution is often used to quantify uncertainties and probability calculus is employed to propagate these uncertainties to prior robust predictions of output quantities of interest (QoI). The measured data collected from system component tests or system operation through monitoring can provide valuable information for improving the mathematical models and the probability models of uncertainties of both the system and loads. Incorporating these data-driven updated models in simulations will yield updated or posterior robust predictions, constituting improved and more reliable estimates of the system performance. However, the computational science tools for handling uncertainties, based on test/monitoring data, in simulations are conceptually and computationally much more challenging than the conventional computing tools (Oden et al. 2006). The objective of this chapter is to present a comprehensive Bayesian probabilistic framework for uncertainty quantification and propagation (UQ+P) in complex structural dynamics simulations based on test data. Bayesian analysis (Beck and Katafygiotis 1998; Beck 2010; Yuen 2010) provides the logical and computational framework to combine knowledge from test/monitoring data and models in a consistent way. The Bayesian framework exploits the available measured data and any prior information based on engineering experience, to perform the following tasks:

- Identify and select the most probable mathematical models among a competitive family of mathematical models (linear vs. nonlinear models; elastic vs. hysteretic models; friction/impact models; correlation structure of a spatially varying quantities such as modulus of elasticity) introduced to represent the behavior of mechanical components.
- Identify probabilistic models that best account in predictions for the mismatch between model-based predictions and measurements, manifested due to the inadequacy/imperfections of the mechanical models used.

- Calibrate the parametric uncertainties involved in mechanical and prediction error models.
- Propagate uncertainties in simulations for updating robust predictions taking into account the validated models and the calibrated uncertainties, as well as rationally weight the effect of one or more highly probable models promoted by the Bayesian methodology.

A Bayesian probabilistic framework is developed in Sect. 2 for UQ+P in complex structural dynamics simulations using vibration measurements collected during system operation. The Bayesian tools used to carry out the computations are presented in Sect. 3. Such tools include asymptotic approximations presented in Sect. 3.1 and sampling algorithms discussed in Sect. 3.2. Among the sampling algorithms, the TMCMC is applied in this work to perform UQ+P. In Sect. 4, the implementation of the Bayesian framework for UQ+P in structural dynamics is presented. The formulation for linear models based on modal frequencies and mode shapes is given in Sect. 4.1. For nonlinear models, the Bayesian UQ+P formulation is based on either full response time histories or nonlinear frequency response spectra. Details of the formulations are given Sect. 4.2.

The simulations of the structure are performed using high-fidelity complex finite element (FE) models that may combine linear and nonlinear components. For FE models involving hundreds of thousands or even million degrees of freedom and localized nonlinear actions activated during system operation, the computational demands in the Bayesian framework may be excessive. Methods for drastically reducing the computational demands at the system, algorithm, and hardware levels involved in the implementation of Bayesian tools are outlined. Such methods include component mode synthesis techniques, consistent with parameterization, to drastically reduce the models of linear components of systems (Papadimitriou and Papadioti 2013; Jensen et al. 2014), surrogate models (Lophaven et al. 2002) to drastically reduce the number of computationally expensive full model runs (Angelikopoulos et al. 2015), and parallel computing algorithms (Angelikopoulos et al. 2012; Hadjidoukas et al. 2015) to efficiently distribute the computations in available multi-core CPUs.

The applicability, effectiveness, and accuracy of the proposed techniques are demonstrated using high-fidelity linear FE models and field measurements for a motorway bridge. For nonlinear FE models, the effectiveness of the proposed asymptotic approximations and sampling algorithms can be found in Giagopoulos et al. (2006, 2013), Green (2015).

2 Bayesian Uncertainty Quantification and Propagation Framework

Consider a parameterized class M_m of structural dynamics models used to predict various output QoI of a system. Let $\underline{\theta}_m \in R^{N_m}$ be a set of parameters in this model class that need to be estimated using experimental data and $\underline{f}(\underline{\theta}_m|M_m)$ be model predictions

of output QoI given a value of the parameter set $\underline{\theta}_m$. Probability distribution functions (PDF) are used to quantify the uncertainty in the parameters $\underline{\theta}_m$. The probability distribution of the parameter set $\underline{\theta}_m$ quantifies how plausible is each possible value of the model parameters. The user may assign a prior probability distribution $\pi_m(\underline{\theta}_m)$ to the model parameters to incorporate prior information on the values of the model parameters. The structural model and uncertainty propagation algorithms can be used to identify the uncertainty in the prediction of the output QoI. However, the probability distribution $\pi_m(\underline{\theta}_m)$ is subjective based on previous knowledge and user experience.

2.1 Parameter Estimation

In Bayesian inference, the interest lies in updating the probability distribution of the model parameters $\underline{\theta}_m$ based on measurements and then propagate these uncertainties through the structural dynamics model to quantify the uncertainty in the output QoI. For this, let $D \equiv \underline{\hat{y}} = \{\underline{\hat{y}}_r \in R^{N_0}, r = 1, \ldots, m\}$ be a set of observations available from experiments, where N_0 is the number of observations. The Bayesian formulation starts by building a probabilistic model that characterizes the discrepancy between the model predictions $\underline{f}(\underline{\theta}_m|M_m)$ obtained from a particular value of the model parameters $\underline{\theta}_m$ and the corresponding data $\underline{\hat{y}}$. This discrepancy always exists due to measurement, model, and computational errors. An error term $\underline{e}$ is introduced to denote this discrepancy. The observation data and the model predictions satisfy the prediction error equation

$$\underline{\hat{y}} = \underline{f}(\underline{\theta}_m|M_m) + \underline{e} \tag{1}$$

A probabilistic structure for the prediction error should be defined to proceed with the Bayesian calibration. Let M_e be a family of probability model classes for the error term $\underline{e}$. This model class depends on a set of prediction error parameters $\underline{\theta}_e$ to be determined using the experimental data. Similarly to the structural model parameters $\underline{\theta}_m$, the probability distribution $\pi_e(\underline{\theta}_e)$ is also assigned to quantify the possible values of the prediction error parameters $\underline{\theta}_e$.

The Bayesian approach (Beck and Katafygiotis 1998; Beck 2010) to model calibration is used for updating the values of the combined set $\underline{\theta} = (\underline{\theta}_m, \underline{\theta}_e)$ associated with the structural and the prediction error parameters. The parameters $\underline{\theta}_m$ and $\underline{\theta}_e$ can be considered to be independent with prior probability distribution for the combined set given by $\pi(\underline{\theta}|M) = \pi_m(\underline{\theta}_m|M_m)\pi_e(\underline{\theta}_e|M_e)$, where $M = \{M_m, M_e\}$ includes the structural and prediction error model classes. The updated PDF $p(\underline{\theta}|D, M)$ of the parameters $\underline{\theta}$, given the data D and the model class M, results from the application of the Bayes theorem

$$p(\underline{\theta}|D, M) = \frac{p(D|\underline{\theta}, M)\ \pi(\underline{\theta}|M)}{p(D|M)} \tag{2}$$

where $p(D|\underline{\theta}, M)$ is the likelihood of observing the data from the model class and $p(D|M)$ is the evidence of the model, given by the multidimensional integral

$$p(D|M) = \int_{\Theta} p(D|\underline{\theta}, M)\, \pi(\underline{\theta}|M)\, d\underline{\theta} \tag{3}$$

over the space of the uncertain model parameters.

The updated probability distribution of the model parameters depends on the selection of the prediction error $\underline{e}$. Invoking the maximum entropy principle, a normal distribution $\underline{e} \sim N(\underline{\mu}, \Sigma)$, where $\underline{\mu}$ is the mean and Σ is the covariance matrix, is a reasonable choice for the error since the normal distribution is the least informative among all distributions with the specified lowest two moments. The structure imposed on the mean vector $\underline{\mu}$ and the covariance matrix Σ affects the uncertainty in the model parameter estimates. A zero-mean model error is usually assumed so that $\underline{\mu} = \underline{0}$. However, to take into account the bias in the model predictions of the various response quantities involved in $\underline{f}(\underline{\theta}_m|M_m)$ and try to reconcile conflicting predictions, one could introduce a shift in the predictions by taking $\underline{\mu} \neq \underline{0}$. In this case the parameters defining the structure of $\underline{\mu}$ are part of the unknowns in $\underline{\theta}_e$ to be determined by the Bayesian technique. A diagonal matrix is a reasonable choice for the covariance matrix in the case where the components of the prediction error can be considered to be uncorrelated. This holds in the case of uncorrelated measurements in $\underline{\hat{y}}$ and independent components in the prediction vector $\underline{f}(\underline{\theta}_m|M_m)$. As a result, the covariance matrix takes the form $\Sigma = diag(\sigma_r^2 \hat{y}_r^2)$, where the variance parameters σ_r^2 are part of the unknown constants in $\underline{\theta}_e$ to be determined by the Bayesian calibration. In structural dynamics, the effect of prediction error correlation has been investigated and found to affect the results of the model calibration when the sensors are closely located (Simoen et al. 2013b). Depending on the nature of the simulated QoI, alternative prediction error models can also be used.

Using the prediction error equation (1), the measured quantities follow the normal distribution $\underline{\hat{y}} \sim N(\underline{f}(\underline{\theta}_m|D) + \underline{\mu}(\underline{\theta}_e), \Sigma(\underline{\theta}_e))$, where the explicit dependence of $\underline{\mu}(\underline{\theta}_e)$ and $\Sigma(\underline{\theta}_e)$ on $\underline{\theta}_e$ is introduced to point out that the mean and the covariance of the overall normal prediction error model depend only on the model prediction error parameters $\underline{\theta}_e$ and is independent of the structural parameters $\underline{\theta}_m$. Consequently, the likelihood $p(D|\underline{\theta}, M)$ of observing the data follows the multivariable normal distribution given by

$$p(D|\underline{\theta}, M) = \frac{|\Sigma(\underline{\theta}_e)|^{-1/2}}{(2\pi)^{m/2}} \exp\left[-\frac{1}{2} J(\underline{\theta}; M)\right] \tag{4}$$

where

$$J(\underline{\theta}; M) = [\underline{\hat{y}} - \underline{f}(\underline{\theta}_m|M_m) - \underline{\mu}(\underline{\theta}_e)]^T \Sigma^{-1}(\underline{\theta}_e)[\underline{\hat{y}} - \underline{f}(\underline{\theta}_m|M_m) - \underline{\mu}(\underline{\theta}_e)] \tag{5}$$

The selection of the prior distribution affects the posterior distribution of the model parameters for the case of relatively small number of data. Usually a noninformative prior can be used. For example, a uniform distribution of the model parameters does not give any preference to the values of the model parameters given the data. For cases of large number of model parameters where unidentifiability issues may occur, a Gaussian prior can avoid unidentifiability issues and enable the estimation of the model parameters using Bayesian numerical analysis tools, avoiding convergence problems of the gradient and stochastic optimization techniques used in Bayesian asymptotic approximations.

2.2 Model Selection

The Bayesian probabilistic framework can also be used to compare two or more competing model classes and select the optimal model class based on the available data. Consider a family $M_{Fam} = \{M_i,\ i = 1, \ldots, \kappa\}$, of κ alternative, competing, parameterized FE and prediction error model classes, and let $\underline{\theta}_i \in R^{N_{\theta_i}}$ be the free parameters of the model class M_i. The posterior probability $Pr(M_i|D)$ of the i-th model class given the data D is (Beck and Yuen 2004; Yuen 2010)

$$Pr(M_i|D) = \frac{p(D|M_i)\ Pr(M_i)}{p(D|M_{Fam})} \tag{6}$$

where $Pr(M_i)$ is the prior probability and $p(D|M_i)$ is the evidence of the model class M_i. The optimal model class M_{best} is selected as the one that maximizes $Pr(M_i|D)$ given by (6). Model class selection is used to compare between alternative model classes and select the best model class (Muto and Beck 2008). The model class selection can also be used to identify the location and severity of damage (Ntotsios et al. 2009).

2.3 Uncertainty Propagation for Robust Prior and Posterior Predictions

Let q be a scalar output QoI of the system. Prior robust predictions, before the availability of measured data, are derived by propagating the prior uncertainties in the model parameters quantified by the prior PDF $\pi(\underline{\theta}|M)$. Posterior robust predictions of q are obtained by taking into account the updated uncertainties in the model parameters given the measurements D. Let $p(q|\underline{\theta}, M)$ be the conditional probability distribution of q given the values of the parameters. Using the total probability theorem, the prior and posterior robust probability distribution $p(q|M)$ of q, taking into account the model M, is given by (Papadimitriou et al. 2001; Beck and Taflanidis 2013)

$$p(q|M) = \int p(q|\underline{\theta}, M)\, p(\underline{\theta}|M)\, d\underline{\theta} \tag{7}$$

as an average of the conditional probability distribution $p(q|\underline{\theta}, M)$ weighting by the PDF $p(\underline{\theta}|M)$ of the model parameters, where $p(\underline{\theta}|M) \equiv \pi(\underline{\theta}|M)$ for prior estimate in the absence of data, or $p(\underline{\theta}|M) \equiv p(\underline{\theta}|D, M)$ for posterior estimate given the data D, respectively.

Let $G(q; \underline{\theta})$ be a performance measure of the system which depends on the deterministic output QoI $q(\underline{\theta})$. The prior robust performance measure $E[G(q; \underline{\theta})|M)] \equiv E_\pi[G(q; \underline{\theta})|M)]$ or the posterior robust performance measure $E[G(q; \underline{\theta})|M)] \equiv E_p[G(q; \underline{\theta})|D, M)]$ given the data D is

$$E[G(q; \underline{\theta})|M)] = \int G(q; \underline{\theta})\, p(\underline{\theta}|M)\, d\underline{\theta} \tag{8}$$

where $p(\underline{\theta}|M)$ is either the prior PDF $\pi(\underline{\theta}|M)$ or the posterior PDF $p(\underline{\theta}|D, M)$, respectively.

2.3.1 Simplified Measures of Uncertainties in Output QoI

Robust predictions of q that account for the uncertainty in $\underline{\theta}$ are also obtained by simplified measures such as mean and variance ${\sigma_q}^2 = E[q^2(\underline{\theta})] - {m_1}^2 = {m_2}^2 - {m_1}^2$ with respect to $\underline{\theta}$, derived from the first two moments m_k of $q(\underline{\theta})$, $k = 1, 2$, given by the multidimensional integrals

$$m_k = \int [q(\underline{\theta})]^k\, p(\underline{\theta}|M)\, d\underline{\theta} \tag{9}$$

over the uncertain parameter space. The integral (9) is a special case of (8) by selecting $G(q; \underline{\theta}) = [q(\underline{\theta})]^k$. Computational tools for estimating the multidimensional integrals are presented in Sect. 3.

2.3.2 Prior and Posterior Robust Reliability

A more challenging problem in uncertainty propagation is the estimation of rare events. This is important in analyzing system reliability or, its complement, probability of failure, or probability of unacceptable performance. The probability of failure is the probability that one or more output QoI exceed certain threshold levels or more generally as the probability that the system performance falls within a failure domain F defined usually by one or more inequality equations.

Let $Pr(\underline{\theta}|M)$ be the probability of failure of the system conditioned on the value of the parameter set $\underline{\theta}$. The robust prior or robust posterior reliability (Papadimitriou et al. 2001; Beck and Taflanidis 2013) or its complement failure probability is obtained by evaluating the multidimensional probability integral

$$P_F(M) = \int Pr(\underline{\theta}|M)\, p(\underline{\theta}|M)\, d\underline{\theta} \tag{10}$$

where $p(\underline{\theta}|M) \equiv \pi(\underline{\theta}|M)$ for prior probability of failure estimate or $p(\underline{\theta}|M) \equiv p(\underline{\theta}|D, M)$ for posterior estimate given the data D, respectively. Assuming that a set of independent random variables $\underline{\psi}$ are used to quantify input and system uncertainties that are not associated with the ones involved in $\underline{\theta}$, the failure probability can also be written in the form

$$P_F(M) = P_r(\underline{z} \in F|M) = \int I_F(\underline{z})\, p(\underline{z}|M)\, d\underline{z} \tag{11}$$

where $\underline{z} = (\underline{\psi}, \underline{\theta})$ is the augmented set of uncertain parameters, F is a failure region in the augmented parameter space, and I_F is an indicator function which is 1 if $\underline{z} \in F$ and 0 elsewhere over the space of feasible system parameters $\underline{z}$.

3 Bayesian Computational Tools

3.1 Asymptotic Approximations

3.1.1 Posterior PDF

For large enough number of measured data, the posterior distribution of the model parameters in (2) can be asymptotically approximated by a Gaussian distribution (Beck and Katafygiotis 1998)

$$p(\underline{\theta}|D, M) \approx \frac{|C(\hat{\underline{\theta}})|^{-1/2}}{(2\pi)^{N_\theta/2}} \exp\left[-\frac{1}{2}(\underline{\theta} - \hat{\underline{\theta}})^T C^{-1}(\hat{\underline{\theta}})(\underline{\theta} - \hat{\underline{\theta}})\right] \tag{12}$$

centered at the most probable value $\hat{\underline{\theta}}$ of the model parameters obtained by maximizing the posterior PDF $p(\underline{\theta}|D, M)$ or, equivalently, minimizing the function

$$g(\underline{\theta}; M) = -\ln p(\underline{\theta}|D, M) = \frac{1}{2}J(\underline{\theta}; M) + \frac{1}{2}|C(\underline{\theta}_e)| - \ln \pi(\underline{\theta}|M) + \frac{N_\theta}{2} ln(2\pi) \tag{13}$$

with covariance matrix $C(\hat{\underline{\theta}}) = h^{-1}(\hat{\underline{\theta}})$ equal to the inverse of the Hessian $h(\theta) = \underline{\nabla\nabla}^T g(\underline{\theta}, M)$ of the function $g(\underline{\theta}; M)$ in (13) evaluated at the most probable value $\hat{\underline{\theta}}$. This approximation is also known as the Bayesian central limit theorem. The asymptotic result (12), although approximate, provides a good representation of the posterior PDF for a number of applications involving even a relatively small number of data.

The asymptotic approximation (12) fails to provide an adequate representation of the posterior probability distribution in the case of multimodal distributions. To improve on the asymptotic approximation, one needs to identify all modes of the posterior PDF and take them into account in the asymptotic expression by considering a weighted contribution of each mode with weights based on the probability volume of the PDF in the neighborhood of each mode (Beck and Katafygiotis 1998). The weighted estimate is reasonable, provided that the modes are separable. For interacting modes or closely spaced modes this estimate is inaccurate due to overlapping of the regions of high probability volume involved in the interaction. However, implementation problems exists in multimodal cases, due to the inconvenience in estimating all modes of the distribution (Katafygiotis and Beck 1998). Asymptotic approximations have also been introduced to handle the unidentifiable cases (Katafygiotis and Lam 2002; Katafygiotis et al. 2000) manifested for relatively large number of model parameters in relation to the information contained in the data.

3.1.2 Model Selection

For model selection, an asymptotic approximation (Beck and Yuen 2004; Yuen 2010; Papadimitriou and Katafygiotis 2001) based on Laplace method can also be used to give an estimate of the evidence integral in (3) that appears in the model selection equation (6). Substituting this estimate in (6), the final asymptotic estimate for $P(M_i|D)$ is given in the form

$$Pr(M_i|D) = \left(\sqrt{2\pi}\right)^{N_{\theta_i}} \frac{p(D|\hat{\underline{\theta}}_i, M_i)\ \pi(\hat{\underline{\theta}}_i|M_i)}{\sqrt{\det\left[h_i(\hat{\underline{\theta}}_i, M_i)\right]}} \frac{Pr(M_i)}{p(D|M_{Fam})} \tag{14}$$

where $\hat{\underline{\theta}}_i$ is the most probable value of the parameters of the model class M_i and $h_i(\theta) = \underline{\nabla\nabla}^T g_i(\underline{\theta}, M)$ is the Hessian of the function $g_i(\underline{\theta}_i; M_i)$ given in (13) for the model class $M \equiv M_i$. It should be noted that the asymptotic estimate for the probability of a model class M_i can readily be obtained given the most probable value and the Hessian of the particular mode. For the multimodal case the expression (14) can be generalized by adding the contributions from all modes.

3.1.3 Posterior Robust Predictions

For the posterior robust prediction integrals such as (7) or (8) with $p(\underline{\theta}|M) \equiv p(\underline{\theta}|D, M)$, a similar asymptotic approximation can be applied to simplify the integrals. Specifically, substituting the posterior PDF $p(\underline{\theta}|D, M)$ from (2) into (8), one obtains that the robust prediction integral is given by (Papadimitriou et al. 1997, 2001)

$$E[G(q; \underline{\theta})|D, M)] = \frac{1}{p(D|M)} \int G(\underline{\theta}; M)\, p(D|\underline{\theta}, M)\, \pi(\underline{\theta}|M)\, d\underline{\theta} \tag{15}$$

Introducing the function

$$r_G(\underline{\theta}; M) = -\ln[G(\underline{\theta}; M)\, p(D|\underline{\theta}, M)\, \pi(\underline{\theta}|M)] \tag{16}$$

the integral in (15) takes the form of Laplace integral which can be approximated as before in the form

$$\int \exp[-r_G(\underline{\theta})]\, d\underline{\theta} = \frac{\exp[-r_G(\tilde{\underline{\theta}})]\left[\sqrt{2\pi}\right]^{N_\theta}}{\sqrt{\det\left[h_G(\tilde{\underline{\theta}})\right]}} \tag{17}$$

where $\tilde{\underline{\theta}}$ is the value of $\underline{\theta}$ that minimizes the function $r_G(\underline{\theta}; M)$, and $h_G(\tilde{\underline{\theta}}, M)$ is the Hessian of the function $r_G(\underline{\theta}; M)$ evaluated at $\tilde{\underline{\theta}}$. Substituting in (15), using (14) to asymptotically approximate the term $p(D|M)$ and replacing $r_G(\underline{\theta})$ by (16), it can be readily derived that $E[G(q; \underline{\theta})|D, M)]$ is given by the asymptotic approximation (Tierney and Kadane 1986)

$$E[G(q)|D, M)] = G(\tilde{\underline{\theta}}; M)\, \frac{p(D|\tilde{\underline{\theta}}, M)}{p(D|\hat{\underline{\theta}}, M)}\, \frac{\pi(\tilde{\underline{\theta}}|M)}{\pi(\hat{\underline{\theta}}|M)} \sqrt{\frac{\det\left[h(\hat{\underline{\theta}}, M)\right]}{\det\left[h_G(\tilde{\underline{\theta}}, M)\right]}} \tag{18}$$

The error in the asymptotic estimate is of order N^{-2}, i.e., inversely proportional to the square of the number of data. The asymptotic estimate requires solving two extra optimization problems, one for the mean and one for the variance of $G(q; \underline{\theta})$. In general, one needs to carry out $2N_q$ extra-optimization problems, where N_q is the number of output quantities of interest. Such optimization problems are independent and can be performed in parallel.

Similarly, the asymptotic approximation can be applied to provide an estimate for the posterior robust probability distribution $p(q|D, M)$ of q defined in (7) for $p(\underline{\theta}|M) \equiv p(\underline{\theta}|D, M)$, the posterior PDF. However, asymptotic approximations are not applicable in the case of computing the robust reliability integral (11). Instead, sampling algorithms can be used in this case as will be discussed in Sect. 3.2.

3.1.4 Gradient-Based Optimization Algorithms

The optimization problems that arise in the asymptotic approximations are solved using available single-objective optimization algorithms. The optimization of $g(\underline{\theta}; M)$ given in (13) and the optimization of $r_G(\underline{\theta}; M)$ given in (16) with respect to $\underline{\theta}$ can readily be carried out numerically using any available algorithm for optimizing a nonlinear function of several variables. In particular, iterative gradient-based optimization algorithms can be conveniently used to achieve fast convergence to the optimum. However, to guarantee the convergence of the gradient-based algorithms for models involving a relatively large number of DOFs, analytical equations for the gradients of the response QoI involved in the objective functions $g(\underline{\theta}; M)$ and $r_G(\underline{\theta}; M)$ are required. The computational effort scales with the number of parameters in $\underline{\theta}$.

Adjoint methods provide a computationally very effective way to estimate the gradients of the objective function with respect to all parameters by solving a single adjoint problem, making the computational effort independent of the number of variables in the set $\underline{\theta}$. A review of a model nonintrusive adjoint method for the case of Bayesian UQ based on modal frequencies and modeshapes is given in Ntotsios and Papadimitriou (2008). For nonlinear models of structures, the techniques for computing gradients of the objectives with respect to the parameters are model intrusive, requiring tedious algorithmic and software development that in most cases are not easily integrated within the commercial software packages. Selected examples of model intrusiveness includes the sensitivity formulation for hysteretic-type nonlinearities in structural dynamics and earthquake engineering (Barbato et al. 2007; Barbato and Conte 2005). The adjoint formulation requires considerable algorithmic development time to set up the equations for the adjoint problem and implement this formulation in software. Moreover, there are cases of systems and type of nonlinearities (e.g., contact, sliding and impact) where the development of an adjoint formulation or analytical equations for the sensitivity of objective functions to parameters is not possible. Derivative-free techniques such as evolution strategies are more appropriate to use in such cases.

3.1.5 Stochastic Optimization Algorithms

Stochastic optimization algorithms are random search algorithms that explore better the parameter space for detecting the neighborhood of the global optimum, avoiding premature convergence to a local optimum. In addition, stochastic optimization algorithms do not require the evaluation of the gradient of the objective function with respect to the parameters. Thus, they are model nonintrusive since there is no need to formulate the equations for the derivatives either by direct or adjoint techniques. Despite their slow convergence, evolutionary strategies are highly parallelizable so the time-to-solution in a HPC environment is often comparable to conventional gradient-based optimization methods (Hadjidoukas et al. 2015).

Stochastic optimization algorithms can be used with parallel computing environments to find the optimum for non-smooth functions or for models for which an adjoint formulation is not possible to develop. Examples include hysteretic models of structural components, as well as problems involving contact, sliding, and impact. In the absence of a HPC environment, the disadvantage of the stochastic optimization algorithms arises from the high number of system reanalyses which may make the computational effort excessive for real-world problems for which a simulation may take minutes, hours, or even days to complete.

A parallelized version of the covariance matrix adaptation evolutionary strategy (CMA-ES) (Hansen et al. 2003) can be used to solve the single-objective optimization problems arising in the Bayesian asymptotic approximations. The CMA-ES algorithm exhibits fast convergence properties among several classes of evolutionary algorithms, especially when searching for a single global optimum. The Hessian estimation required in Bayesian asymptotic approximations can be computed using the Romberg method (Lyness and Moler 1969). This procedure is based on a number of system reanalyses at the neighborhood of the optimum, which can all be performed independently for problems involving either calibration or propagation, and are thus highly parallelizable. Details can be found in Hadjidoukas et al. (2015).

3.2 Sampling Algorithms

In contrast to asymptotic approximations, sampling algorithms are nonlocal methods capable of providing accurate representations for the posterior PDF and accurate robust predictions of output QoI. Sampling algorithms, such as Markov Chain Monte Carlo (MCMC) (Metropolis et al. 1953; Hastings 1970; Cheung and Beck 2009) are often used to generate samples $\underline{\theta}^{(i)}$, $i = 1, \ldots, N$, for populating the posterior PDF in (2), estimating the model evidence and computing the uncertainties in output QoI. Among the stochastic simulation algorithms available, the transitional MCMC algorithm (TMCMC) (Ching and Chen 2007) is one of the most promising algorithms for finding and populating with samples the important region of interest of the posterior probability distribution, even in challenging unidentifiable cases and multimodal posterior distributions. Approximate methods based on Kernels are then used to estimate marginal distributions of the parameters. In addition, the TMCMC method yields an estimate of the evidence in (3) of the model class M_i based on the samples already generated by the algorithm.

Sampling methods can be conveniently used to estimate the multidimensional integrals (7) and (8) from the samples $\underline{\theta}^{(i)}, i = 1, \ldots, N$, generated from the posterior probability distribution $p(\underline{\theta}|D, M)$. In this case, the integrals (7) and (8) can be approximated by the sample estimates

$$p(q|M) \approx \frac{1}{N}\sum_{i=1}^{N} p(q|\theta^{(i)}, M) \tag{19}$$

$$E[G(q;\underline{\theta})|M)] \approx \frac{1}{N}\sum_{i=1}^{N} G(q;\underline{\theta}^{(i)}) \tag{20}$$

respectively. The simplified measures of uncertainties given in (9) are also given by the sample estimate (20) with $G(q;\underline{\theta}) = [q(\underline{\theta})]^k$. The sample estimates (19) and (20) require independent forward system simulations that can be executed in a perfectly parallel fashion.

3.2.1 Parallel TMCMC in HPC Environment

HPC techniques are used to reduce the time-to-solution of TMCMC algorithm at the computer hardware level. The TMCMC algorithm is very-well suited for parallel implementation in a computer cluster. Details of the parallel implementation are given in Angelikopoulos et al. (2012), Hadjidoukas et al. (2015). Specifically, a parallel implementation algorithm is activated at every stage of the TMCMC algorithm exploiting the large number of short, variable length, chains that need to be generated at the particular TMCMC stage. Dynamic scheduling schemes can be conveniently used to optimally distribute these chains in a multihost configuration of complete heterogeneous computer workers. The dynamic scheduling scheme ensures an efficient balancing of the loads per computer worker in the case of variable run time of likelihood function evaluations and unknown number of surrogates activated during estimation. Specifically, each worker is periodically interrogated at regular time intervals by the master computer about its availability and samples from TMCMC chains are submitted to the workers on a first-come first-serve basis to perform the likelihood function evaluations so that the idle time of the multiple workers is minimized. It should be noted that uncertainty propagation using sampling algorithms is highly parallelizable. For infinite computing resources, the time-to-solution for making robust prediction of a number of response QoI can be of the order of the time-to-solution for one simulation run. The parallelized version of the TMCMC algorithm for Bayesian UQ has been implemented in software and is available in http://www.cse-lab.ethz.ch/software/Pi4U.

3.2.2 Parallel Subset Simulation in HPC Environment For Robust Prior and Posterior Reliability

For rare events, the subset simulation SubSim (Au and Beck 2011) is computationally the most efficient sampling algorithm to provide an accurate estimate of the multidimensional failure probability integral (11) with the fewest number of samples. The SubSim was first introduced to handle the conditional probability of failure integrals

$F(\underline{\theta})$ formulated by (11) with $\underline{z} = \underline{\psi}$ and then the robust prior reliability integral (11) with $\underline{z} = (\underline{\psi}, \underline{\theta})$ and $p(\underline{z}|M) = p(\underline{\psi}|M)\pi(\underline{\theta}|M)$. Certain improvements on the MCMC sampling within SubSim have recently been proposed by Papaioannou et al. (2015).

In Jensen et al. (2013), SubSim was extended to treat the robust posterior reliability integrals of the form (11) with $\underline{z} = (\underline{\psi}, \underline{\theta})$ and $p(\underline{z}|M) = p(\underline{z}|D, M)$, the posterior PDF. It should be noted that usually due to independence between $\underline{\psi}$ and $\underline{\theta}$, the PDF of $\underline{z}$ is $p(\underline{z}|M) = p(\underline{\psi}|M)p(\underline{\theta}|D, M)$ which simplifies the evaluation of the integral with SubSim (Jensen et al. 2013). SubSim is highly parallelizable and its parallel implementation for heterogeneous architectures is discussed in Hadjidoukas et al. (2015).

4 Implementation in Structural Dynamics

In structural dynamics the formulation of the likelihood in (2) depends on the models and type of measurements used. Details in the implementation of the Bayesian framework for the linear and nonlinear model cases are presented next, separately for each model case and measurements available.

4.1 Uncertainty Quantification of Linear Models in Structural Dynamics

For linear models of structures the quantification of the uncertainties in the model parameters is often based on identified modal frequencies and mode shapes at the locations where sensors are placed. Details on the formulation of the likelihood in (2) can be found in a number of published papers (Vanik et al. 2000; Yuen et al. 2006; Simoen et al. 2013a, b; Christodoulou and Papadimitriou 2007; Goller et al. 2012).

4.1.1 Likelihood Formulation Based on Modal Properties

To apply the Bayesian formulation for parameter estimation of linear FE models, we consider that the data D consist of the square of the modal frequencies, $\hat{\lambda}_r = \hat{\omega}_r^2$, and the mode shapes $\hat{\underline{\phi}}_r \in R^{N_{0,r}}$, $r = 1, \ldots, m$, experimentally estimated using vibration measurements, where m is the number of identified modes and $N_{0,r}$ is the number of measured components for mode r. Usually, it is convenient to measure the vibration of the structure under operational conditions by placing sensors at various locations to measure output only response time histories. There are a number of techniques for estimating the modal frequencies and mode shapes from output only vibration measurements. Notable is the Bayesian modal parameter estimation method proposed in Au (2012). In addition to the most probable values of the modal characteristics, the

uncertainty in these characteristics is also estimated and asymptotically approximated by Gaussian distributions.

Consider a parameterized linear FE model class M of a structure and let $\underline{\theta} \in R^{N_\theta}$ be a vector of free structural model parameters to be estimated using a set of modal properties identified from vibration measurements. Let $\omega_r(\underline{\theta})$ and $\underline{\phi}_r(\underline{\theta})^{N_{0,r}}$ be the r-th modal frequency and modeshape at $N_{0,r}$ DOF, respectively, predicted by the model for a given value of the $\underline{\theta}$ of the model parameters. The likelihood $p(D|\underline{\theta}, M)$ in (2) is built up using the following considerations. The prediction error equation for the r-th modal frequency is introduced

$$\hat{\omega}_r^2 = \omega_r^2(\underline{\theta}) + \varepsilon_{\lambda_r} \tag{21}$$

where ε_{λ_r} is the model error taken to be Gaussian with zero mean and standard deviation $\sigma_{\omega_r}\hat{\omega}_r$, with the unknown parameter σ_{ω_r} to be included in the parameter set $\underline{\theta}_e$ to be estimated.

The prediction error equation for the r-th mode shape is

$$\hat{\underline{\phi}}_r = \beta_r(\underline{\theta})\underline{\phi}_r(\underline{\theta}) + \underline{\varepsilon}_{\underline{\phi}_r} \tag{22}$$

where $\underline{\varepsilon}_{\underline{\phi}_r}$ is the model error taken to be Gaussian with zero mean and covariance matrix $diag(\sigma^2_{\phi_r}||\hat{\underline{\phi}}_r||^2)$, with the unknown $\sigma^2_{\underline{\phi}_r}$ to be included in the parameter set to be estimated, and $\beta_r(\underline{\theta}) = \hat{\underline{\phi}}_r^T \underline{\phi}_r(\underline{\theta}) / \left\| \underline{\phi}_r(\underline{\theta}) \right\|^2$ is a normalization constant that guaranties that the measured mode shape $\hat{\underline{\phi}}_r$ at the measured DOF is closest to the model mode shape $\beta_r(\underline{\theta})\underline{\phi}_r(\underline{\theta})$ predicted by the particular value of $\underline{\theta}$, and $||\underline{z}||^2 = \underline{z}^{\mathrm{T}}\underline{z}$ is the usual Euclidian norm.

The squares of the modal frequencies $\lambda_r(\underline{\theta}) = \omega_r^2(\underline{\theta})$ and the mode shape components $\underline{\phi}_r(\underline{\theta}) = L_r\underline{\varphi}_r(\underline{\theta}) \in \mathbb{R}^{N_{0,r}}$ at the N_0 measured DOF are computed from the full mode shapes $\underline{\varphi}_r(\underline{\theta}) \in \mathbb{R}^n$ that satisfy the eigenvalue problem

$$[K(\underline{\theta}) - \lambda_r(\underline{\theta})M(\underline{\theta})]\underline{\varphi}_r(\underline{\theta}) = \underline{0} \tag{23}$$

where $K(\underline{\theta}) \in \mathbb{R}^{n\times n}$ and $M(\underline{\theta}) \in \mathbb{R}^{n\times n}$ are, respectively, the stiffness and mass matrices of the FE model of the structure, n is the number of model DOF, and $L_r \in R^{N_{0,r}\times n}$ is an observation matrix, usually comprised of zeros and ones, that maps the n model DOF to the $N_{0,r}$ observed DOF for mode r. For a model with large number of DOF, $N_{0,r} \ll n$.

The structural model class M is augmented to include the prediction error model class that postulates zero-mean Gaussian models for the modal frequency and mode shape error terms ε_{λ_r} and $\underline{\varepsilon}_{\underline{\phi}_r}$ in (22) and (23), respectively, with equal variances σ^2 for all modal frequency errors ε_{λ_r} and equal variances σ^2/w for all mode shape errors

$\varepsilon_{\underline{\phi}_r}$. Assuming $\sigma^2_{\omega_r} = \sigma^2$ and $\sigma^2_{\underline{\phi}_r} = \sigma^2_{\omega_r}/w = \sigma^2/w$, the likelihood function can then readily obtained in the form

$$p(D|\underline{\theta}, M) = \frac{1}{\left(\sqrt{2\pi}\sigma\right)^{m(N_0+1)}} \exp\left[-\frac{1}{2\sigma^2} J(\underline{\theta}; w)\right] \tag{24}$$

where

$$J(\underline{\theta}; w) = J_1(\underline{\theta}) + wJ_2(\underline{\theta}) \tag{25}$$

In (25) the following modal frequency residuals

$$J_1(\underline{\theta}) = \sum_{r=1}^{m} \varepsilon^2_{\lambda_r}(\underline{\theta}) = \sum_{r=1}^{m} \frac{[\lambda_r(\underline{\theta}) - \hat{\lambda}_r]^2}{\hat{\lambda}_r^2} \tag{26}$$

and mode shape residuals

$$J_2(\underline{\theta}) = \sum_{r=1}^{m} \varepsilon^2_{\underline{\phi}_r}(\underline{\theta}) = \sum_{r=1}^{m} \frac{\left\| \beta_r(\underline{\theta})\underline{\phi}_r(\underline{\theta}) - \hat{\underline{\phi}}_r \right\|^2}{\left\| \hat{\underline{\phi}}_r \right\|^2} \tag{27}$$

measure the differences ε_{λ_r} and $\varepsilon_{\underline{\phi}_r}$ for the modal frequencies and mode shape components between the identified modal data and the model predicted modal data, respectively. It is worth noting that it can be shown that the square of the modeshape residuals in (27) is related to the modal assurance criterion (MAC) value of the mode r by Papadimitriou et al. (2011)

$$\varepsilon^2_{\underline{\phi}_r}(\underline{\theta}) = 1 - MAC_r^2(\underline{\theta}) = 1 - \left[\frac{\left[\underline{\phi}_r\right]^T \hat{\underline{\phi}}_r}{\left\|\underline{\phi}_r\right\| \left\|\hat{\underline{\phi}}_r\right\|} \right]^2 \geq 0 \tag{28}$$

since $0 \leq MAC_r^2 \leq 1$. Thus $J_2(\underline{\theta})$ in (27) is also a measure of the distance of the square MAC value from one, or equivalently, a measure of the correlation of the model predicted mode shape and the measured mode shape.

4.1.2 Model Reduction, Surrogate, and Parallelization

The Bayesian tools for identifying FE models as well as performing robust prediction analyses require a moderate to very large number of repeated system analyses to be performed over the space of uncertain parameters. Consequently, the computational demands depend highly on the number of system analyses and the time required for

performing a system analysis. For linear FE models with large number of DOFs, this can increase substantially the computational effort to excessive levels. In addition, computational savings are achieved by adopting parallel computing algorithms to efficiently distribute the computations in available multi-core CPUs (Angelikopoulos et al. 2012; Hadjidoukas et al. 2015). Specifically, the Π4U software (Hadjidoukas et al. 2015), based on a parallelized version of the Transitional MCMC (TMCMC) algorithm, can be used to efficiently distribute the computations in available multi-core CPUs. Moreover, X-TMCMC methods (Angelikopoulos et al. 2015) that include kriging within TMCMC can also be used to replace the full system simulations by fast approximations, reducing by an order of magnitude the number of full system reanalyses.

In structural dynamics, fast and accurate component mode synthesis (CMS) techniques, consistent with the finite element (FE) model parameterization, can be integrated with Bayesian techniques to reduce efficiently and drastically the model and thus the computational effort (Papadimitriou and Papadioti 2013; Jensen et al. 2014). Model reductions techniques (Papadimitriou and Papadioti 2013; Goller et al. 2011) can achieve reductions of the size of the stiffness and mass matrices by several orders of magnitude. In particular, computational efficient model reduction techniques based on component mode synthesis have been developed recently to handle certain parameterization schemes for which the mass and stiffness matrices of a component depend either linearly or nonlinearly on only one of the free model parameters to be updated, often encountered in FE model updating formulations. In such schemes, it has been shown that the repeated solutions of the component eigenproblems are completely avoided, reducing substantially the computational demands, without compromising the solution accuracy. For the case of linear and nonlinear dependence of the stiffness matrix of a structural component on a model parameter, the methodology is presented in Papadimitriou and Papadioti (2013) and Jensen et al. (2014, 2015). The model reduction methods are applicable to both asymptotic and stochastic simulation tools used in Bayesian framework.

4.1.3 Gradient Estimation and Adjoint Techniques

For Bayesian asymptotic approximations, first-order and second-order adjoint techniques have been developed (Ntotsios and Papadimitriou 2008) using the Nelson's method (Nelson 1976) to efficiently compute the required first- and second-order sensitivities in the optimization problems and the Hessian computations. In Nelson method the gradient of the modal frequencies and the modeshape vector of a specific mode are computed from only the value of the modal frequency and the modeshape vector of the same mode, independently of the values of the modal frequencies and modeshape vectors of the rest of the modes. For structural model classes with large number of degrees of freedom and very few contributing modes, this representation of the gradients clearly presents significant computational advantages over methods that represent modeshape gradients as a weighted, usually arbitrarily truncated, sum of all system modeshape vectors (Fox and Kapoor 1968). Specifically, following

(Ntotsios and Papadimitriou 2008), the gradient of the square error $\varepsilon^2_{\lambda_r}(\underline{\theta})$ in (26) is given by

$$\frac{\partial \varepsilon^2_{\lambda_r}(\underline{\theta})}{\partial \theta_j} = \frac{\partial \varepsilon^2_{\lambda_r}(\underline{\theta})}{\partial \lambda_r}\frac{\partial \lambda_r}{\partial \theta_j} = \left[\frac{\partial \varepsilon^2_{\lambda_r}(\underline{\theta})}{\partial \lambda_r}\underline{\varphi}_r^T\right](K_j - \omega_r^2 M_j)\underline{\varphi}_r \tag{29}$$

and the gradient of the square error $\varepsilon^2_{\underline{\phi}_r}(\underline{\theta})$ in (27) is given by

$$\frac{\partial \varepsilon^2_{\underline{\phi}_r}(\underline{\theta})}{\partial \theta_j} = -\left[\underline{x}_r^T(I - M\underline{\varphi}_r\underline{\varphi}_r^T)\right](K_j - \omega_r^2 M_j)\underline{\varphi}_r \tag{30}$$

where $\underline{x}_r$ is given by the solution of the linear system of equations

$$A_r^{*T}\underline{x}_r = L^T \nabla_{\underline{\varphi}_r}\varepsilon^2_{\underline{\varphi}_r}(\underline{\theta}) \tag{31}$$

with

$$\frac{\partial \varepsilon^2_{\lambda_r}(\underline{\theta})}{\partial \lambda_r} = \frac{2\varepsilon_{\omega_r}(\underline{\theta})}{\hat{\omega}_r^2} \tag{32}$$

$$\nabla^T_{\underline{\varphi}_r}\varepsilon^2_{\underline{\varphi}_r}(\underline{\theta}) = \frac{2\varepsilon_{\underline{\varphi}_r}(\underline{\theta})\beta_r}{\left\|\hat{\underline{\varphi}}_r\right\|} \tag{33}$$

while $K_j \equiv \partial K/\partial\theta_j$ and $M_j \equiv \partial M/\partial\theta_j$. In (31), the matrix A_r^* is used to denote the modified matrix derived from $A_r = K - \omega_r^2 M$ by replacing the elements of the k-th column and the k-th row by zeroes and the (k,k) element of A_r by one, where k denotes the element of the modeshape vector $\underline{\phi}_r$ with the highest absolute value (Nelson 1976).

The computation of the derivatives of the square errors for the modal properties of the r-th mode with respect to the parameters in $\underline{\theta}$ requires only one solution of the linear system (31), independent of the number of parameters in $\underline{\theta}$. For a large number of parameters in the set $\underline{\theta}$, the above formulation for the gradient of the mean error in modal frequencies given in (29) and the gradient of the mean error of the modeshape components in $\underline{\theta}$ is computationally very efficient and informative. The dependence on θ_j comes through the term $K_j - \omega_r^2 M_j$ and the term M_j. For the case where the mass matrix is independent of $\underline{\theta}$, $M_j = 0$ the formulation is further simplified. The end result of the proposed adjoint method is the solution of as many linear systems of equations as the number of model predicted modes. The size of the linear systems equals the number of the DOFs of the structural model which adds to the computational burden. However, the linear systems are independent of each other and can be carried out in parallel, significantly accelerating the time-to-solution. The

integration of model reduction techniques with the adjoint methods can be found in Papadimitriou and Papadioti (2013).

It should be noted that for the special case of linear dependence between the global mass and stiffness matrices on the parameters in the set $\underline{\theta}$, that is, $M(\underline{\theta}) = M_0 + \sum_{j=1}^{N_\theta} M_j \theta_j$ and $K(\underline{\theta}) = K_0 + \sum_{j=1}^{N_\theta} K_j \theta_j$, the gradients of $M(\underline{\theta})$ and $K(\underline{\theta})$ are easily computed from the reduced constant matrices M_0, K_0, M_j and K_j, $j = 1, \ldots, N_\theta$. In order to save computational time, these constant matrices are computed and assembled once and, therefore, there is no need this computation to be repeated during the iterations involved in optimization algorithms. For the general case of nonlinear dependence between the global mass and stiffness matrices on the parameters in the set $\underline{\theta}$, the matrices M_j and K_j involved in the formulation can be obtained numerically at the element level and assembled to form the global matrices.

It should be noted that a similar analysis exists for obtaining the Hessian of the objective functions $\varepsilon^2_{\omega_r}(\underline{\theta})$ and $\varepsilon^2_{\underline{\varphi}_r}(\underline{\theta})$ from the second derivatives of the eigenvalues and the eigenvectors, respectively. Details can be found in Ntotsios and Papadimitriou (2008).

4.2 *Uncertainty Quantification of Nonlinear Models In Structural Dynamics*

The nonlinearities in structural dynamics arise from various sources, including material constitutive laws, contact, sliding, and impact between structural components, nonlinear isolation devices such as nonlinear dampers in civil infrastructure and nonlinear suspension models in vehicles. In a number of structural dynamics cases, the nonlinearities are localized in isolated parts of a structure, while the rest of the structure behaves linearly. Such localized nonlinearities can be found in vehicles where the frame usually behaves linearly and the nonlinearities are activated at the suspension mainly due to the dampers. In civil engineering structures, the nonlinearities are at some cases localized at the various structural elements (dampers, etc.) introduced to isolate the structure during system operation.

For nonlinear models of structures the quantification of the uncertainties in the model parameters depends on the measured quantities that are available. The likelihood function $p(D|\underline{\theta}, M)$ in (2) is formulated based on either full response time histories or frequency response spectra.

4.2.1 Likelihood Formulation Based on Response Time Histories

To apply the Bayesian formulation for parameter calibration of both linear and nonlinear models, we consider that the data consists of measured time histories $D = \left\{\hat{x}_j(k) \in R,\ j = 1, \ldots, N_0,\ k = 1, \ldots, N_D\right\}$ at time instances $t = k\Delta t$, of N_0 response quantities (displacements, accelerations and forces) at different points in

the structure, where N_D is the number of the samples data using a sampling period Δt. Let also $\left\{x_j(k;\underline{\theta}) \in R, j = 1,\ldots,N_0,\ k = 1,\ldots,N_D\right\}$ be the predictions of the response time histories for the same quantities and points in the structure, from the nonlinear model corresponding to a particular value of the parameter set $\underline{\theta}$. The measured and the model predicted response time history measurements satisfy for each time instant k the prediction error equations

$$\hat{x}_j(k) = x_j(k;\underline{\theta}) + e_j(k) \tag{34}$$

$j = 1,\ldots,N_0$ and $k = 1,\ldots,N_D$. The difference between the measured and model predicted response is attributed to both experimental and modeling errors.

The prediction errors $e_j(k)$, measuring the fit between the measured and the model predicted response time histories, are modeled by Gaussian distributions. The likelihood formulation depends on the user postulation of the correlation structure of the prediction errors in (34). Herein, it is assumed that the model prediction errors are uncorrelated in time. At different time instants the terms $e_j(k)$ are assumed to be independent zero-mean Gaussian variables with equal variances for all sampling data of a response time history, i.e., $e_j(k) \sim N(0,\sigma_j^2)$. Each measured time history is generally obtained from a different sensor (displacement, acceleration or force sensor) with a different accuracy and noise level, giving rise to as many prediction error variances σ_j^2 as the number of measured time histories. The prediction error parameters $\sigma_j, j = 1,\ldots,N_0$, are contained in the prediction error vector $\underline{\sigma} \in R^{N_0}$. Herein, the prediction error parameters are considered unknown and are included in the parameters to be calibrated given the data, along with the structural model parameters in the set $\underline{\theta}$. The likelihood formulation for model prediction errors that are correlated in time using autoregressive (AR) models to quantify such correlation is presented in Christodoulou (2006).

The likelihood function $p\left(D|\underline{\theta},M\right)$, which quantifies the probability of obtaining the data given a specific set of structural parameters and prediction error parameters, is derived by noting that the measured time histories $\hat{x}_j\,(k)$ are independent Gaussian variables with mean $x_j\left(k;\underline{\theta}\right)$ and variance σ_j^2. Taking advantage of the independence of the measured quantities both at different time instants of the same time history as well as between different time histories, the likelihood takes the form

$$p\left(D|\underline{\theta},M\right) = \prod_{j=1}^{N_0}\prod_{k=1}^{N_D} p\left(\hat{x}_j\,(k)\,|\underline{\theta}\right) \tag{35}$$

Substituting with the Gaussian PDF for $p\left(\hat{x}_j\,(k)\,|\underline{\theta}\right)$ and rearranging terms one obtains that

$$p\left(D|\underline{\theta},M\right) = \frac{1}{\left(\sqrt{2\pi}\right)^{N_D N_0}\prod_{j=1}^{N_0}\sigma_j^{N_D}} \exp\left\{-\frac{N_0 N_D}{2} J\left(\underline{\theta}\right)\right\} \tag{36}$$

where

$$J\left(\underline{\theta}\right) = \frac{1}{N_0} \sum_{j=1}^{N_0} \frac{1}{\sigma_j^2} J_j\left(\underline{\theta}\right) \tag{37}$$

with

$$J_j\left(\underline{\theta}\right) = \frac{1}{N_D} \sum_{k=1}^{N_D} \left[\hat{x}_j\left(k\right) - x_j\left(k; \underline{\theta}\right)\right]^2 \tag{38}$$

represents the measure of fit between the measured and the model predicted response time history for response quantity j.

Formulations of the likelihood for the case where full measured response time histories are available can be found in Metallidis et al. (2003), Metallidis and Natsiavas (2008). The likelihood and the posterior of the parameters of a FE model are functions of the response time histories predicted by the FE model. Each posterior evaluation requires the integration of the linear or nonlinear set of equations of motion.

4.2.2 Likelihood Based on Nonlinear Response Spectra

The formulation of the likelihood for the case where frequency response spectra are available, can be found in Giagopoulos et al. (2013). To apply the Bayesian formulation for parameter estimation of nonlinear models based on frequency response spectra, we consider that the data consists of measured response spectra $D = \left\{\underline{\hat{s}}_j(k) \in R^{N_o}, j = 1, \ldots, N_0, k = 1, \ldots, N_D\right\}$ of N_o response quantities (displacement, velocity, acceleration strain) at different DOF and at different frequencies ω_k, where k is a frequency index and N is the number of sampled data in the frequency domain. In addition, let $\left\{s_j(k; \underline{\theta}_m) \in R^{N_o}, j = 1, \ldots, N_0, k = 1 \ldots, N_D\right\}$ be the model response predictions of frequency response spectra, corresponding to the DOFs where measurements are available, given the model class M and the parameter set $\underline{\theta}_m \in R^{N_\theta}$. It is assumed that the observation data and the model predictions satisfy the prediction error equation

$$\hat{s}_j(k) = s_j(k; \underline{\theta}_m) + e_j(k) \tag{39}$$

It is assumed that the error terms $e_j(k)$ are independent, both at different frequencies of the same response spectra as well as between response spectra measured at different locations, an assumption that is very reasonable for the case that the measured data consists of frequency response spectra. In addition, the error term $e_j(k)$ is assumed to be Gaussian vector with mean zero and variance σ_j^2, independent of k.

Using (39) it follows that the measured quantity $\hat{s}_j(k)$ is a Gaussian distribution with mean $s_j(k;\underline{\theta}_m)$ and variance σ_j^2.

Taking advantage of the independence of the prediction errors, the likelihood $p(D|\underline{\theta}, M)$ is formulated as follows:

$$p\left(D|\underline{\theta}\right) = \prod_{j=1}^{N_0}\prod_{k=1}^{N} p\left(\hat{s}_j\left(k\right)|\underline{\theta}\right) \tag{40}$$

Using the Gaussian probability density function for $s_j(k;\underline{\theta}_m)$ and substituting in (40), one obtains the likelihood function in the form (36) where measure of fit $J\left(\underline{\theta}\right)$ between the measured and the model predicted response spectra is given by (37) with

$$J_j\left(\underline{\theta}\right) = \frac{1}{N_D}\sum_{k=1}^{N}\left[\hat{s}_j\left(k\right) - s_j\left(k;\underline{\theta}\right)\right]^2 \tag{41}$$

It is clear that the likelihood and the posterior of the model parameters are functions of the frequency response spectra predicted by the FE model. Each posterior evaluation requires the integration of the nonlinear set of equation of motion of the structure for as many different number of harmonic excitations as the number of frequency response spectra ordinates. This, however, increases substantially the computational effort.

4.2.3 Model Reduction, Surrogates, and Parallelization

Model reduction techniques based on CMS are readily applicable for special class of problems where the nonlinearities are localized at isolated parts of the structure. In such cases the structure can be decomposed into linear and nonlinear components and the dynamic behavior of the linear components be represented by reduced models. An implementation of such framework can be found in Jensen et al. (2014, 2015) where it is demonstrated that substantial reductions in the DOFs of the model can be achieved which eventually yield reductions in computational effort for performing a simulation run without sacrificing the accuracy. Surrogate estimates are also applicable to reduce the number of full system analyses in sampling techniques such as TMCMC. The X-TMCMC algorithm (Angelikopoulos et al. 2015) can be used within parallelized TMCMC in HPC environments (Hadjidoukas et al. 2015) to reduce the computational effort by one order of magnitude by replacing full system analyses by approximate kriging estimates. For the case where the measurements are given as full response time histories, the surrogate estimates are applied to approximate the value of the log posterior PDF. For the case where the measurements consist of nonlinear frequency response spectra, it is more convenient computationally to apply the surrogate estimates for each spectral ordinate of the spectrum (Giagopoulos

et al. 2013). In addition, in the latter case, it should be pointed out that another parallelization level can be introduced in which the frequency response spectral values can run in parallel, taking advantage of HPC environments to speed up computations (Hadjidoukas et al. 2015).

4.2.4 Gradient Estimation

For Bayesian asymptotic approximations, analytical approximations of the gradients of objective functions are not readily available. The development time and software implementation may be substantial. For certain classes of hysteretic nonlinearities, formulations for the sensitivities of the response quantities to parameter uncertainties have been developed (Barbato et al. 2007) and can be used within the Bayesian framework. However, it should be pointed out that such formulation are model intrusive and are not easily integrated to commercial computer software packages available for simulating nonlinear structural dynamics problems. For the model cases where adjoint techniques can be applied, the development time may also be substantial. However, for a number of important nonlinear class of models (e.g., impact, hysteretic) or output QoI such as frequency response spectra, adjoint methods are not applicable. The absence of sensitivity estimates or adjoint formulations may substantially increase the computational cost and/or render gradient-based optimization algorithms unreliable for use with Bayesian asymptotic approximation tools. Stochastic optimization and stochastic simulations algorithms within a HPC environment (Hadjidoukas et al. 2015) are, respectively, the preferred algorithms to be used with Bayesian asymptotic and stochastic simulation tools.

5 Application

The Bayesian framework for UQ+P is demonstrated for linear structural dynamics applications by developing a high-fidelity FE models of the Metsovo bridge using modal characteristics identified from ambient vibration measurements. These models are representative of the initial structural condition of the bridge and can be further used for structural health monitoring purposes and for updating structural reliability and safety. The purpose of the present application is mainly to demonstrate the Bayesian UQ framework and the computational effectiveness of proposed model reduction technique based on CMS. The efficiency of the surrogate techniques based on kriging method introduced within the sampling algorithm TMCMC has been explored in Angelikopoulos et al. (2015). The capabilities of the parallelization procedures has been reported in Hadjidoukas et al. (2015). The application of the Bayesian UQ+P framework in nonlinear models using time histories and frequency response spectra can be found elsewhere (Giagopoulos et al. 2006, 2013; Green et al. 2015; Green 2015; Jensen et al. 2014, 2015).

5.1 *Metsovo Bridge Description, Instrumentation, and Modal Identification*

The Metsovo bridge, shown in Fig. 1, is the highest reinforced concrete bridge of the Egnatia Motorway, with the height of the tallest pier equal to 110 m. The total length of the bridge is 537 m. The bridge has 4 spans of length 44.78, 117.87, 235, 140 m and 3 piers of which the left pear (45 m) supports the boxbeam superstructure through pot bearings (movable in both horizontal directions), while the central (110 m) and the right (35 m) piers connect monolithically to the structure. The total width of the deck is 13.95 m, for each carriageway. The superstructure is limited prestressed of single boxbeam section, of height varying from 4.00 to 13.5 m. The central and the right piers are founded on huge circular 12.0 m rock sockets in a depth of 25 and 15 m, respectively.

Acceleration measurements were collected under normal operating conditions of the bridge in order to identify the modal properties of the structure (natural frequencies, mode shapes, damping ratios). The measured data were collected using 5 triaxial and 3 uniaxial accelerometers paired with a 24-bit data logging system and an internal SD flash card for data storage. The synchronization of the sensors was achieved using a GPS module in each of the sensors. The excitation of the bridge during the measurements was primarily due to road traffic, which ranged from motorcycles to heavy trucks, and environmental excitation such as wind loading and ground microtremor.

Given the limited number of sensors and the large length of the deck, multiple sets of measurements are performed in order to identify the type of the modes accurately. Specifically, 13 sensor configurations are used to cover the entire length of the deck. The sensors are located approximately 20 m apart. Each measurement lasted 20 min with a sampling rate of 200 Hz. The reference sensors, consisting of one triaxial and three uniaxial sensors (one vertical and two horizontal), one at each side of the bridge. Their purpose is to provide common measurement points along different configurations in order to assemble the mode shapes (Au 2010; Yan and Katafygiotis 2015). The locations of the reference sensors was obtained by minimizing the information

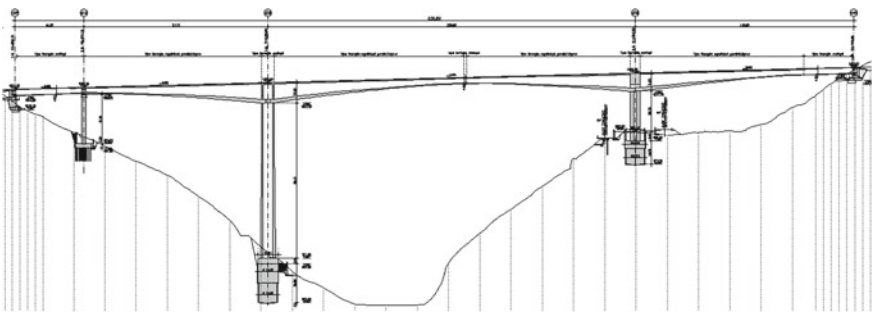

Fig. 1 Metsovo bridge

entropy using an optimal sensor location theory (Papadimitriou and Lombaert 2012; Yuen and Kuok 2015) so as to provide the highest information content for identifying the modal parameters of the structure.

Following a Bayesian identification methodology (Au 2012) and a mode shape assembling algorithm (Au 2010), the natural frequencies and damping ratios of the structure were extracted, and the mode shape components of each configuration were combined to produce the full mode shapes of the structure at all 159 sensor locations covered by the 13 configurations. For comparison purposes, Table 1 presents the mean and the standard deviation of the experimentally identified modal frequencies for the lowest 10 modes of the Metsovo bridge. Representative assembled mode shapes are shown in Fig. 2 and compared with the mode shapes predicted by the nominal FE model of the bridge.

Table 1 Experimentally identified (EXP) and model predicted mean (MOD) modal frequencies, as well as MAC values between experimentally identified and model predicted modeshapes

Mode	Type	EXP mean	EXP std	Nominal	MOD mean	MAC mean
1	Transverse	0.306	0.0007	0.318	0.290	0.9988
2	Transverse	0.603	0.0014	0.622	0.581	0.9841
3	Bending	0.623	0.0008	0.646	0.641	0.9983
4	Transverse	0.965	0.0084	0.989	0.816	0.9989
5	Bending	1.047	0.0066	1.112	1.088	0.9965
6	Transverse	1.139	0.0049	1.173	1.117	0.9997
7	Bending	1.428	0.0042	1.516	1.446	0.9589
8	Transverse	1.697	0.0112	1.711	1.573	0.9981

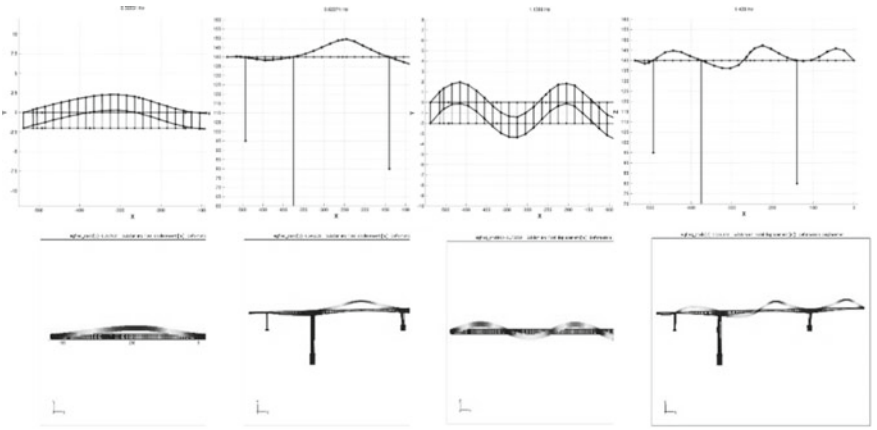

Fig. 2 Experimentally identified and model predicted mode shapes *left* to *right* first transverse, first bending, fourth transverse, third bending

5.2 Finite Element Model of Bridge

Two classes of FE models are created using three-dimensional tetrahedron quadratic Lagrange finite elements. The first model is a fixed-base finite element model. The nominal values of the modulus of elasticity of the deck and the three piers were selected to be the values used in design. A coarse FE mesh is chosen to predict the lowest 20 modal frequencies and mode shapes of the bridge with sufficient accuracy. The largest size of the elements in the mesh is of the order of the thickness of the deck cross section. This model has 562,101 DOFs and is used next to check in detail the model reduction technique and its effectiveness in terms of size reduction and accuracy.

The second model takes into account the soil–structure interaction by modeling the soil with large blocks of material and embedding the piers and abutments into these blocks. The nominal values of the soil stiffness was selected based on design values. A large uncertainty in this values was reported from soil tests. Several mesh sizes were tried, and an accuracy analysis was performed in order to find a reasonable trade-off between the number of degrees of freedom of the model and the accuracy in modal frequencies. By trying different mesh sizes in the deck, piers, and soil blocks, a mesh of 830.115 DOFs was kept for the bridge–foundation–soil structure model. This mesh was found to cause errors of the order of 0.1–0.5 % in the first 20 modal frequencies, compared to the smallest possible mesh sizes which had approximately 3 million DOFs. In that way the model was optimized with respect to the number of DOFs using a variable element size in each part of the bridge. This can be noted especially in Fig. 3 where the size of the elements grows larger in the soil blocks.

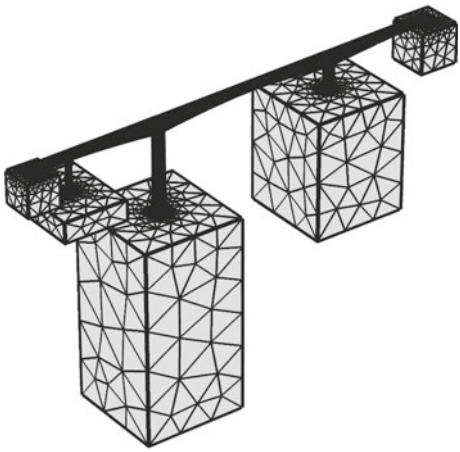

Fig. 3 Finite element mesh of the bridge with the soil blocks

5.3 Model Reduction Based on CMS

Model reduction is used to reduce the model and thus the computational effort to manageable levels. Specifically, the parameterization-consistent component mode synthesis (CMS) technique is applied. To demonstrate the effectiveness of the model reduction technique, the fixed-base FE model of the bridge is considered, ignoring the soil stiffness.

Let ω_c be the cutoff frequency which represents the highest modal frequency that is of interest in FE model updating. Herein, the cutoff frequency is selected to be equal to the 20th modal frequency of the nominal model, i.e., $\omega_c = 4.55$ Hz. For demonstration purposes, the bridge is divided into nine physical components with eight interfaces between components as shown in Fig. 4. For each component it is selected to retain all modes that have frequency less than $\omega_{\max} = \rho\omega_c$, where the ρ values affect the computational efficiency and accuracy of the CMS technique. The total number of internal DOFs before the model reduction is applied and the number of modes retained for various ρ values are given in Table 2. For the case $\rho = 8$, a total of 286 internal modes out of the 558,801 are retained for all nine components. The total number of DOFs of the reduced model is 3,586 which also includes 3,300 constraint interface DOFs for all components. It is clear that a two orders of magnitude reduction in the number of DOFs is achieved using CMS. Table 2 also shows the fractional error between the modal frequencies computed using the complete FE model and the ones computed using the CMS technique for $\rho = 2$, 5, and 8. It is seen that the error fall below 0.02 % for $\rho = 8$, 0.17 % for $\rho = 5$ and 1.10 % for $\rho = 2$. A very good accuracy is achieved for the case of $\rho = 5$.

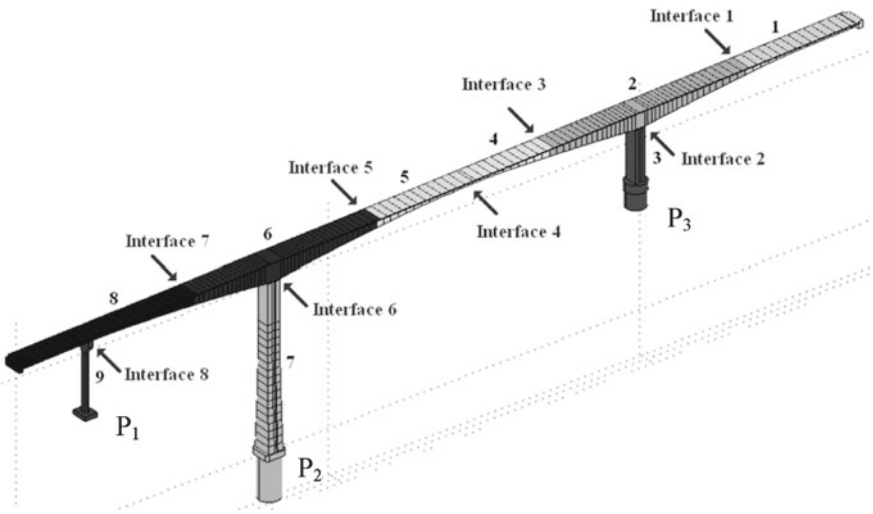

Fig. 4 Components of FE model of the bridge

Table 2 Number of DOF and percentage modal frequency error for the full (unreduced) and reduced models

DOF	Full model	$\rho = 8$	$\rho = 5$	$\rho = 2$	$\rho = 8$ $\nu = 200$	$\rho = 5$ $\nu = 200$	$\rho = 2$ $\nu = 200$
Internal	558,801	286	100	31	286	100	31
Interface	3,300	3,300	3,300	3,300	306	306	306
Total	562,101	3,586	3,400	3,331	592	406	337
Highest percentage error (%)	0.00	0.02	0.17	1.10	0.20	0.30	1.20

The large number of the interface DOFs can be reduced by retaining only a fraction of the constrained interface modes (Papadimitriou and Papadioti 2013). For each interface, only the modes that have frequency less than $\omega_{\max} = \nu\omega_c$ are retained, where ν is user and problem dependent. Results for $\nu = 200$ are given in Table 2. It can be seen that the fractional error for the lowest 20 modes of the structure fall below 1.20 % for $\nu = 200$. In particular, for $\nu = 200$ and $\rho = 5$ the reduced system has 406 DOFs from which 100 generalized coordinates are fixed-interface modes for all components and the rest 306 generalized coordinates are constrained interface modes. The error in this cases falls below 0.3 %.

Thus, using CMS a drastic reduction in the number of generalized coordinates is obtained which can exceed three orders of magnitude, without sacrificing the accuracy with which the lowest model frequencies are computed. The time-to-solution for one run of the reduced model is of the order of a few seconds which should be compared to approximately 2 min required for solving the unreduced FE model.

5.4 Uncertainty Calibration of Bridge FE Model

The FE model of the bridge–foundation–soil system is next calibrated based on the experimentally identified modal frequencies and the formulation presented in Sect. 4.1 for $w = 1$. Model reduction was performed using the same structural components as the ones used for the fixed-base bridge model. In addition five more structural components were used that correspond to the five rectangular soil blocks added to model the flexibility of the soil. The reduced FE model using only reduction in the internal DOF with $\rho = 5$ has 16205 DOF, while the reduced FE model with internal and interface DOF reduction has 1.891 DOF, corresponding to two to three orders reduction in DOF.

The FE model of the bridge–foundation–soil system is parameterized using three parameters associated with the modulus of elasticity of one or more structural components. Specifically, the first parameter θ_1 accounts for the modulus of elasticity of the deck, components 1, 2, 4, 5, 6, and 8 of the bridge as shown in Fig. 4. The second parameter θ_2 accounts for the modulus of elasticity of the three piers (components 3,

7, and 9), assumed to be perfectly correlated, while the third parameter θ_3 accounts for the modulus of elasticity of the soil, assumed to be the same at all bridge supports. The model parameters in the set $\underline{\theta}$ scale the nominal values of the properties that they model. The lowest eight modal frequencies of the left branch of Metsovo bridge predicted by the nominal model are presented in Table 1 and are compared to the modal frequencies estimated using the ambient vibration measurements.

The prior distribution was assumed to be uniform with bounds in the domain $[0.2, 2] \times [0.2, 2] \times [0.01, 10]$ for the structural model parameters and in the domain $[0.001, 1]$ for the prediction error parameter σ. The domain for the soil parameter was deliberately chosen larger in order to account for the large uncertainty in the values of the soil stiffness reported in the design and be able to explore the full effect of the soil stiffness on the model behavior.

The calibration is done using the lowest 8 modal frequencies and mode shapes identified for the structure. Representative results are obtained using the TMCMC for the bridge–foundation–soil FE model with the three structural model parameters. The TMCMC is used to generate samples from the posterior PDF of the structural model and prediction error parameters and then the uncertainty is propagated to estimate the uncertainty in the modal frequencies of the bridge. 1000 samples per TMCMC stage are used, resulting to a total number of approximately 10000 model simulation runs. The updated marginal distributions of the model parameters are shown in Fig. 5. It can be seen that the value of the most uncertain parameter prior to the data, the soil stiffness, is approximately 0.4 times the nominal value with small uncertainty of the order of 2 %. The updated most probable values of the deck and pier stiffness are estimated to be approximately 1.12 and 1.02 the nominal values, with uncertainties of the order of 3 % and 11 %, respectively.

The mean of the updated uncertainty in the first 8 modal frequencies and MAC values between the experimentally identified and model predicted modeshapes are presented in Table 1. The predictions of the mean values are overall closer to the experimental data than the values predicted from the nominal model. However, there is a trade-off in the fit, according to which a number of the calibrated modal frequencies become closer to the experimental ones, while a number of them move further away from the experimental modal frequencies. The overall fit between the experimental and the model predicted modal characteristics is summarized in Fig. 6 which shows the frequency fits and the mode shape fits using the MAC values.

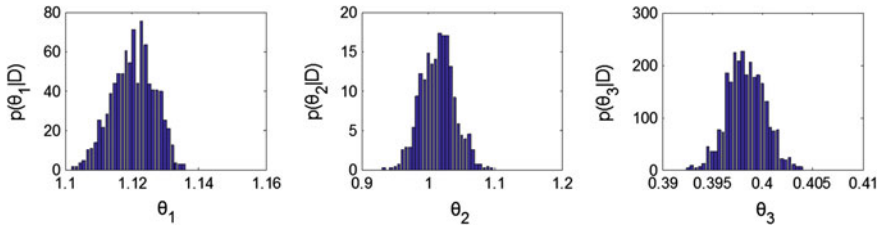

Fig. 5 Marginal posterior distribution of model parameters. (1) Deck, (2) piers, (3) soil

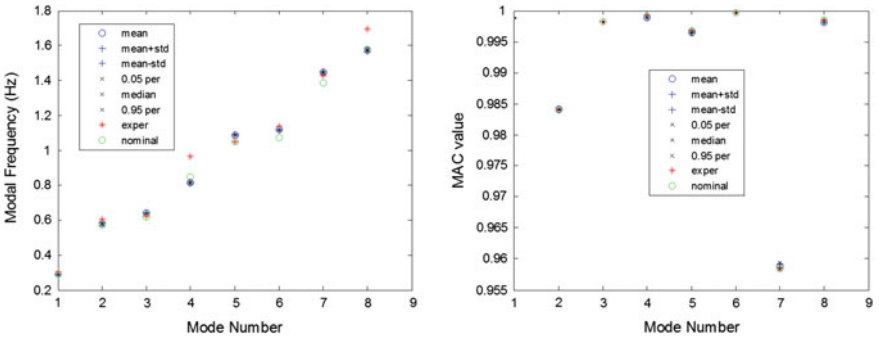

Fig. 6 *Left* Frequency fits, *right* MAC values between measured and model predicted mode shapes

5.5 Computational Issues

The model nonintrusive TMCMC algorithm used within Bayesian tools for model parameter uncertainty quantification and calibration of the Metsovo bridge requires a moderate to large number of approximately 10000 FE model simulation runs. For the large-order FE model developed for the Metsovo bridge with hundreds of thousands DOFs, the computational demands involved are excessive due to the several minutes required to compete one model simulation run. From the computational point of view, the analyses can be performed using model reduction, surrogate models, and the parallelized TMCMC using the Π4U software (Hadjidoukas et al. 2015). Model reduction techniques drastically reduce size of the FE model by two to three orders of magnitude, from a little less than a million DOFs to a couple of thousand DOFs. Surrogate models reduce the number of model reanalyses by one order of magnitude (Angelikopoulos et al. 2015). The reduction in computing time also scales linearly with the number of available cores when parallel computing algorithms are activated. Herein the analysis was performed in a 4-core double-threaded computer using the model reduction technique. Overall more than four orders of magnitude reduction in computational time was achieved in performing the model updating. The time-to-solution is approximately 8–9 min, four orders of magnitude less than the time required for the full model run in a sequentially computing environment.

6 Conclusions

A Bayesian framework was presented for estimating the uncertainties in the structural and prediction error model parameters, selecting the best models of structural components among competing alternatives, and propagating uncertainties for robust response and reliability predictions. Asymptotic approximations and sampling algorithms were proposed for Bayesian UQ+P. In Bayesian asymptotic approximations,

gradient-based optimization algorithms require the availability of direct model output sensitivity analyses or more efficient adjoint techniques. Gradient-free stochastic optimization algorithms such as CMA-ES are highly parallelizable and competitive alternatives when a HPC environment is available. In Bayesian sampling techniques, the TMCMC and the kriging-based X-TMCMC are highly parallelizable algorithms that can be used in a HPC environment to efficiently distribute the large number of independent system simulations in available multi-core CPUs. Such techniques have been implemented in the Π4U software (Hadjidoukas et al. 2015) that can be downloaded from http://www.cse-lab.ethz.ch/software/Pi4U.

The implementation of the framework in structural dynamics was outlined for linear structural models using experimental identified modal frequencies and mode-shapes, as well as for nonlinear structural models using either measured response time histories or frequency response spectra. To efficiently handle large-order models of hundreds of thousands or millions degrees of freedom, and localized nonlinear actions activated during system operation, fast and accurate component mode synthesis (CMS) techniques, consistent with the finite element model parameterization, are employed that achieve drastic reductions in the model order and the computational effort. Surrogate models based on the kriging techniques and implemented within X-TMCMC are also used to substantially speed up computations by up to one order of magnitude, avoiding full reanalyses of the unreduced or reduced models.

It is demonstrated with an application on a full-scale bridge that these HPC and model reduction techniques, integrated within Bayesian tools, can be effective in calibrating the uncertainty of FE models with hundred of thousands DOF, achieving drastic reductions in computational effort by more than three orders of magnitude. The integration of model reduction techniques, surrogate models and HPC within Bayesian uncertainty quantification and propagation tools can result in drastic reduction of computational time to manageable levels for complex models used for simulations of structural dynamics and related engineering systems.

Acknowledgments The chapter summarizes research implemented under the ARISTEIA Action of the Operational Programme Education and Lifelong Learning and co-funded by the European Social Fund (ESF) and Greek National Resources.

References

Angelikopoulos, P., Papadimitriou, C., Koumoutsakos, P. (2012). Bayesian uncertainty quantification and propagation in molecular dynamics simulations: A high performance computing framework. *Journal of Chemical Physics*, *137*(14).

Angelikopoulos, P., Papadimitriou, C., & Koumoutsakos, P. (2015). X-TMCMC: Adaptive kriging for Bayesian inverse modeling. *Computer Methods in Applied Mechanics and Engineering*, *289*, 409–428.

Au, S. K. (2010). Assembling mode shapes by least squares. *Mechanical Systems and Signal Processing*, *25*, 163–179.

Au, S. K. (2012). Fast Bayesian ambient modal identification in the frequency domain, part II: Posterior uncertainty. *Mechanical Systems and Signal Processing*, *26*, 76–90.

Au, S. K., & Beck, J. L. (2011). Estimation of small failure probabilities in high dimensions by subset simulation. *Probabilistic Engineering Mechanics*, *16*, 263–277.

Barbato, M., & Conte, J. P. (2005). Finite element response sensitivity analysis: A comparison between force-based and displacement-based frame element models. *Computer Methods in Applied Mechanics and Engineering*, *194*(12–16), 1479–1512.

Barbato, M., Zona, A., & Conte, J. P. (2007). Finite element response sensitivity analysis using three-field mixed formulation: General theory and application to frame structures. *International Journal for Numerical Methods in Engineering*, *69*(1), 114–161.

Beck, J. L. (2010). Bayesian system identification based on probability logic. *Structural Control and Health Monitoring*, *17*(7), 825–847.

Beck, J. L., & Katafygiotis, L. S. (1998). Updating models and their uncertainties. I: Bayesian statistical framework. *ASCE Journal of Engineering Mechanics*, *124*(4), 455–461.

Beck, J. L., & Taflanidis, A. (2013). Prior and posterior robust stochastic predictions for dynamical systems using probability logic. *International Journal for Uncertainty Quantification*, *3*(4), 271–288.

Beck, J. L., & Yuen, K. V. (2004). Model selection using response measurements: Bayesian probabilistic approach. *ASCE Journal of Engineering Mechanics*, *130*(2), 192–203.

Cheung, S. H., & Beck, J. L. (2009). Bayesian model updating using hybrid Monte Carlo simulation with application to structural dynamic models with many uncertain parameters. *ASCE Journal of Engineering Mechanics*, *135*(4), 243–255.

Ching, J. Y., & Chen, Y. C. (2007). Transitional Markov chain Monte Carlo method for Bayesian model updating. *Model Class Selection, and Model Averaging*, *133*(7), 816–832.

Christodoulou, K. (2006). Development of damage detection and identification methodology. PhD Thesis, University of Thessaly.

Christodoulou, K., & Papadimitriou, C. (2007). Structural identification based on optimally weighted modal residuals. *Mechanical Systems and Signal Processing*, *21*(1), 4–23.

Fox, R. L., & Kapoor, M. P. (1968). Rate of change of eigenvalues and eigenvectors. *AIAA Journal*, *6*(12), 2426–2429.

Giagopoulos, D., Salpistis, C., & Natsiavas, S. (2006). Effect of nonlinearities in the identification and fault detection of gear-pair systems. *International Journal of Non-Linear Mechanics*, *41*, 213–230.

Giagopoulos, D., Papadioti, D.-C., Papadimitriou, C., & Natsiavas, S. (2013). Bayesian uncertainty quantification and propagation in nonlinear structural dynamics. In *International Modal Analysis Conference (IMAC), Topics in Model Validation and Uncertainty Quantification* (pp. 33–41).

Goller, B., Pradlwarter, H. J., & Schueller, G. I. (2011). An interpolation scheme for the approximation of dynamical systems. *Computer Methods in Applied Mechanics and Engineering*, *200*(1–4), 414–423.

Goller, B., Beck, J. L., & Schueller, G. I. (2012). Evidence-based identification of weighting factors in Bayesian model updating using modal data. *ASCE Journal of Engineering Mechanics*, *138*(5), 430–440.

Green, P. L. (2015). Bayesian system identification of a nonlinear dynamical system using a novel variant of simulated annealing. *Mechanical Systems and Signal Processing*, *52*, 133–146.

Green, P. L., Cross, E. J., & Worden, K. (2015). Bayesian system identification of dynamical systems using highly informative training data. *Mechanical Systems and Signal Processing*, *56*, 109–122.

Hadjidoukas, P. E., Angelikopoulos, P., Papadimitriou, C., & Koumoutsakos, P. (2015). 4U: A high performance computing framework for Bayesian uncertainty quantification of complex models. *Journal of Computational Physics*, *284*(1), 1–21.

Hansen, N., Muller, S. D., & Koumoutsakos, P. (2003). Reducing the time complexity of the derandomized evolution strategy with covariance matrix adaptation (CMA-ES). *Evolutionary Computation*, *11*(1), 1–18.

Hastings, W. K. (1970). Monte-Carlo sampling methods using Markov chains and their applications. *Biometrika*, *57*(1), 97–109.

Jensen, H. A., Vergara, C., Papadimitriou, C., & Millas, E. (2013). The use of updated robust reliability measures in stochastic dynamical systems. *Computer Methods in Applied Mechanics and Engineering*, *267*, 293–317.

Jensen, H. A., Millas, E., Kusanovic, D., & Papadimitriou, C. (2014). Model-reduction techniques for Bayesian finite element model updating using dynamic response data. *Computer Methods in Applied Mechanics and Engineering*, *279*, 301–324.

Jensen, H. A., Mayorga, F., & Papadimitriou, C. (2015). Reliability sensitivity analysis of stochastic finite element models. *Computer Methods in Applied Mechanics and Engineering*, *296*, 327–351.

Katafygiotis, L. S., & Beck, J. L. (1998). Updating models and their uncertainties. II: Model identifiability. *ASCE Journal of Engineering Mechanics*, *124*(4), 463–467.

Katafygiotis, L. S., & Lam, H. F. (2002). Tangential-projection algorithm for manifold representation in unidentifiable model updating problems. *Earthquake Engineering and Structural Dynamics*, *31*(4), 791–812.

Katafygiotis, L. S., Lam, H. F., & Papadimitriou, C. (2000). Treatment of unidentifiability in structural model updating. *Advances in Structural Engineering—An International Journal*, *3*(1), 19–39.

Lophaven, S. N., Nielsen, H. B., & Sndergaard, J. (2002). *DACE,A MATLAB Kriging Toolbox*. DTU: DK-2800 Kgs.

Lyness, J. N., & Moler, C. B. (1969). Generalized Romberg methods for integrals of derivatives. *Numerische Mathematik*, *14*(1), 1–13.

Metallidis, P., & Natsiavas, S. (2008). Parametric identification and health monitoring of complex ground vehicle models. *Journal of Vibration and Control*, *14*(7), 1021–1036.

Metallidis, P., Verros, G., Natsiavas, S., & Papadimitriou, C. (2003). Fault detection and optimal sensor location in vehicle suspensions. *Journal of Vibration and Control*, *9*(3–4), 337–359.

Metropolis, N., Rosenbluth, A. W., Rosenbluth, M. N., Teller, A. H., & Teller, E. (1953). Equation of state calculations by fast computing machines. *The Journal of Chemical Physic*, *21*(6), 1087–1092.

Muto, M., & Beck, J. L. (2008). Bayesian updating and model class selection for hysteretic structural models using stochastic simulation. *Journal of Vibration and Control*, *14*(1–2), 7–34.

Nelson, R. B. (1976). Simplified calculation of eigenvector derivatives. *AIAA Journal*, *14*(9), 1201–1205.

Ntotsios, E., & Papadimitriou, C. (2008). Multi-objective optimization algorithms for finite element model updating. In *Proceedings of International Conference on Noise and Vibration Engineering (ISMA)* (pp. 1895–1909).

Ntotsios, E., Papadimitriou, C., Panetsos, P., Karaiskos, G., Perros, K., & Perdikaris, P. C. (2009). Bridge health monitoring system based on vibration measurements. *Bulletin of Earthquake Engineering*, *7*(2), 469–483.

Oden, J. T., Belytschko, T., Fish, J., Hughes, T. J. R., Johnson, C., Keyes, D., et al. (2006). *Simulation-Based Engineering Science (SBES) Revolutionizing Engineering Science through Simulation*. Report of the NSF: Blue Ribbon Panel on SBES.

Papadimitriou, C., & Katafygiotis, L. S. (2001). A Bayesian methodology for structural integrity and reliability assessment. *International Journal of Advanced Manufacturing Systems*, *4*(1), 93–100.

Papadimitriou, C., & Lombaert, G. (2012). The effect of prediction error correlation on optimal sensor placement in structural dynamics. *Mechanical Systems and Signal Processing*, *28*, 105–127.

Papadimitriou, C., & Papadioti, D. C. (2013). Component mode synthesis techniques for finite element model updating. *Computers and Structures*, *126*, 15–28.

Papadimitriou, C., Beck, J. L., & Katafygiotis, L. S. (1997). Asymptotic expansions for reliability and moments of uncertain dynamic systems. *ASCE Journal of Engineering Mechanics*, *123*(12), 1219–1229.

Papadimitriou, C., Beck, J. L., & Katafygiotis, L. S. (2001). Updating robust reliability using structural test data. *Probabilistic Engineering Mechanics*, *16*(2), 103–113.

Papadimitriou, C., Ntotsios, E., Giagopoulos, D., & Natsiavas, S. (2011). Variability of updated finite element models and their predictions consistent with vibration measurements. *Structural Control and Health Monitoring*, *19*(5), 630–654.

Papaioannou, I., Betz, W., Zwirglmaier, K., & Straub, D. (2015). MCMC algorithms for subset simulation. *Probabilistic Engineering Mechanics*, *41*, 89–103.

Simoen, E., Moaveni, B., Conte, J. L., & Lombaert, G. (2013a). Uncertainty quantification in the assessment of progressive damage in a 7-story full-scale building slice. *ASCE Journal of Engineering Mechanics*, *139*(12), 1818–1830.

Simoen, E., Papadimitriou, C., & Lombaert, G. (2013b). On prediction error correlation in Bayesian model updating. *Journal of Sound and Vibration*, *332*(18), 4136–4152.

Tierney, L., & Kadane, J. B. (1986). Accurate approximations for posterior moments and marginal densities. *Journal of the American Statistical Association*, *81*(393), 82–86.

Vanik, M. W., Beck, J. L., & Au, S. K. (2000). Bayesian probabilistic approach to structural health monitoring. *ASCE Journal of Engineering Mechanics*, *126*(7), 738–745.

Yan, W.-J., & Katafygiotis, L. S. (2015). A novel Bayesian approach for structural model updating utilizing statistical modal information from multiple setups. *Structural Safety*, *52*(Part B), 260–271.

Yuen, K.-V. (2010). *Bayesian methods for structural dynamics and civil engineering*. Wiley.

Yuen, K.-V., & Kuok, S.-C. (2015). Efficient Bayesian sensor placement algorithm for structural identification: A general approach for multi-type sensory systems. *Earthquake Engineering and Structural Dynamics*, *44*(5), 757–774.

Yuen, K. V., Beck, J. L., & Katafygiotis, L. S. (2006). Efficient model updating and health monitoring methodology using incomplete modal data without mode matching. *Structural Control and Health Monitoring*, *13*(1), 91–107.